Ecological Indicators 109 (2020) 105756

Contents lists available at ScienceDirect

Ecological Indicators

journal homepage: www.elsevier.com/locate/ecolind

Original Articles

Urbanization increased river nitrogen export to western Taiwan Strait despite increased retention by nitrification and denitrification

Jingjie Lin[a,b], Nengwang Chen[a,b,*], Fenfang Wang[b], Zhenyu Huang[b], Xinyu Zhang[b], Lei Liu[b]

[a] State Key Laboratory of Marine Environmental Science, Xiamen University, Xiamen, China
[b] Fujian Provincial Key Laboratory for Coastal Ecology and Environmental Studies, College of the Environment and Ecology, Xiamen University, Xiamen, China

ARTICLE INFO

Keywords:
Nitrogen pollution
Urbanization
Eutrophication
River

ABSTRACT

Urban development and increased human activities impose major environmental stress on the receiving bodies of water. Although urban rivers have been recognized as hotspots of regional nitrogen (N) pollution, detailed measurements of river nutrient species in response to urbanization are rarely reported, so the impacts of urban development on N cycling processes and transport to coast remains unclear. Here we investigated the changes in N species (concentration, composition and isotope) and N functional genes between upstream and downstream sections of several rivers affected by urban development in western Taiwan Strait under various flow conditions (low, medium and high flow). Our results suggest that urban sewage (high ammonium) is the predominant substrate that stimulated nitrification and subsequently denitrification and gaseous N removal (N_2O, N_2). Nitrifying and denitrifying functional genes increased their abundance along the urban rivers. There were hydrological and meteorological controls on urban rivers regulating changes in nitrogen retention between seasons. Overall, the enhanced microbe-driven N retention could not balance the increase of urban N loading. Consequently, urbanization increased riverine N export and caused other changes in nutrient supply such as changing the nutrient ratio (N:P:Si ratio), increasing the potential for eutrophication both in the river and in receiving coastal ecosystems.

1. Introduction

Global human population and urban development are increasing and as a result impose major environmental stress on the receiving bodies of water (Duha et al., 2008). Dense urban areas produce large amounts of nutrient pollution, which are often discharged into local rivers. These polluted rivers transport nutrient enriched waters which ultimately can cause eutrophication, harmful algal blooms (HABs), hypoxia and other ecological problems in downstream, in estuaries and ultimately in the adjacent coastal areas (Chen and Hong, 2012; Paerl et al., 2016). By 2030, more than 60% of the global population will be living in urban areas (Duh et al., 2008; FAO, 2018). The urbanization rate in China has increased from 52.6% to 58.5% since 2014 (Li, 2018). Urban areas in China have experienced rapid land use change (Seto and Fragkias, 2005), and economic activities and vulnerable ecosystems often converge in coastal areas (de Andres et al., 2017). Continuing urbanization in coastal regions has increased anthropogenic emissions of reactive nitrogen (N) (Xian et al., 2019) and changed N retention capacity which is the rate of nitrogen cycled among aquatic biota, benthic sediments and water column (Dalu et al., 2019; Marce et al., 2018). A better understanding of the relationships between coastal urbanization and ecosystem is vital to develop mitigation strategies to achieve environmental sustainability.

Urban waste discharge affects nitrogen biogeochemical cycles (Grimm et al., 2008). In Shanghai, China, a long-term (1952–2004) impact of urbanization on N inputs was mainly attributed to fossil fuel combustion, Haber-Bosch N fixation and food/feed import (Gu et al., 2012). Mass fluxes and $\delta^{15}N$ signatures revealed that sewage was the predominant nutrient source in the Haihe catchment that includes the megacity of Beijing (Pernet-Coudrier et al., 2012). Understanding of the relationship with water quality indicators correlated with the increase in urban population and per capita waste production is critical to urban planning and management (Ding et al., 2016; Hobbie et al., 2017; Panthi et al., 2017). Urban rivers have been recognized as hotspots of regional N pollution (Zhang et al., 2017; Zhang et al., 2015). A scenario-based modeling study in the UK indicated that climate change (rainfall depth and intensity) combined with increasing urbanization is likely to worsen river water quality (dissolved oxygen and ammonium concentrations) (Astaraie-Imani et al., 2012). The interactions between urbanization and variations of environmental quality has been

* Corresponding author at: College of the Environment and Ecology, Xiamen University, Xiamen, Fujian 361102, China.
E-mail address: nwchen@xmu.edu.cn (N. Chen).

https://doi.org/10.1016/j.ecolind.2019.105756
Received 25 May 2019; Received in revised form 12 September 2019; Accepted 18 September 2019
Available online 26 October 2019
1470-160X/

identified (Duha et al., 2008). However, detailed measurements of river nutrient species in response to urbanization are rarely reported, and the impacts of urban development on N cycling, retention and transport to coast remains unclear.

Here we studied the impact of urbanization on N biogeochemical processes and seaward export of N in four urban rivers of different sizes, all located in the western coast of the Taiwan Strait (Southeast China), by conducting comprehensive measurements under different flow conditions in 2017–2018. The specific objectives of the study were: (1) to investigate the changes in river N species (concentration, composition and isotope) and N functional genes passing through urban areas; (2) to examine how urbanization impacts the strength of nitrification and denitrification; and (3) to reveal the hydrological and meteorological controls on urban rivers regulating N retention and seaward export.

2. Materials and methods

2.1. Study area

Four urban rivers of different sizes, all located along the western coast of the Taiwan Strait, were selected for this study (Fig. 1). The section of the river chosen for detailed study was generally a short reach as it passed through an urban area which was relatively close to the discharge of the river to the coast. At present, three wastewater treatment plants (WWTPs) operated in Zhangzhou City of the Jiulong River and most of urban sewage is secondary treated. Other rivers without WWTPs received raw sewage. Summary statistics for river length, drainage area and land use are presented in Table 1. The region has a subtropical monsoon climate with strong seasonal variation in rainfall and temperature. About 70% of precipitation occurs from May to September, and flow condition (discharge) varies with rainfall over the season (Fig. 1S). In the study period (2017–2018) the low flow period (LF) was from October to December and the average air temperature was 19.3 ± 4.8 °C, the medium flow period (MF) was from January to May and the average air temperature was 18.0 ± 5.7 °C, and the high flow period (HF) was from June to September and the average air temperature was 27.5 ± 2.0 °C.

2.2. Sampling campaign

We conducted three samplings on 28 October 2017 (LF), 5 May 2018 (MF) and 28 July 2018 (HF). For each river we chose an upstream (US) and downstream (DS) site in the middle of bridges near to the city. Surface water (0.5 m depth) was collected by a 5 L plexiglass sampler. Dissolved oxygen (DO), water temperature and pH were measured in

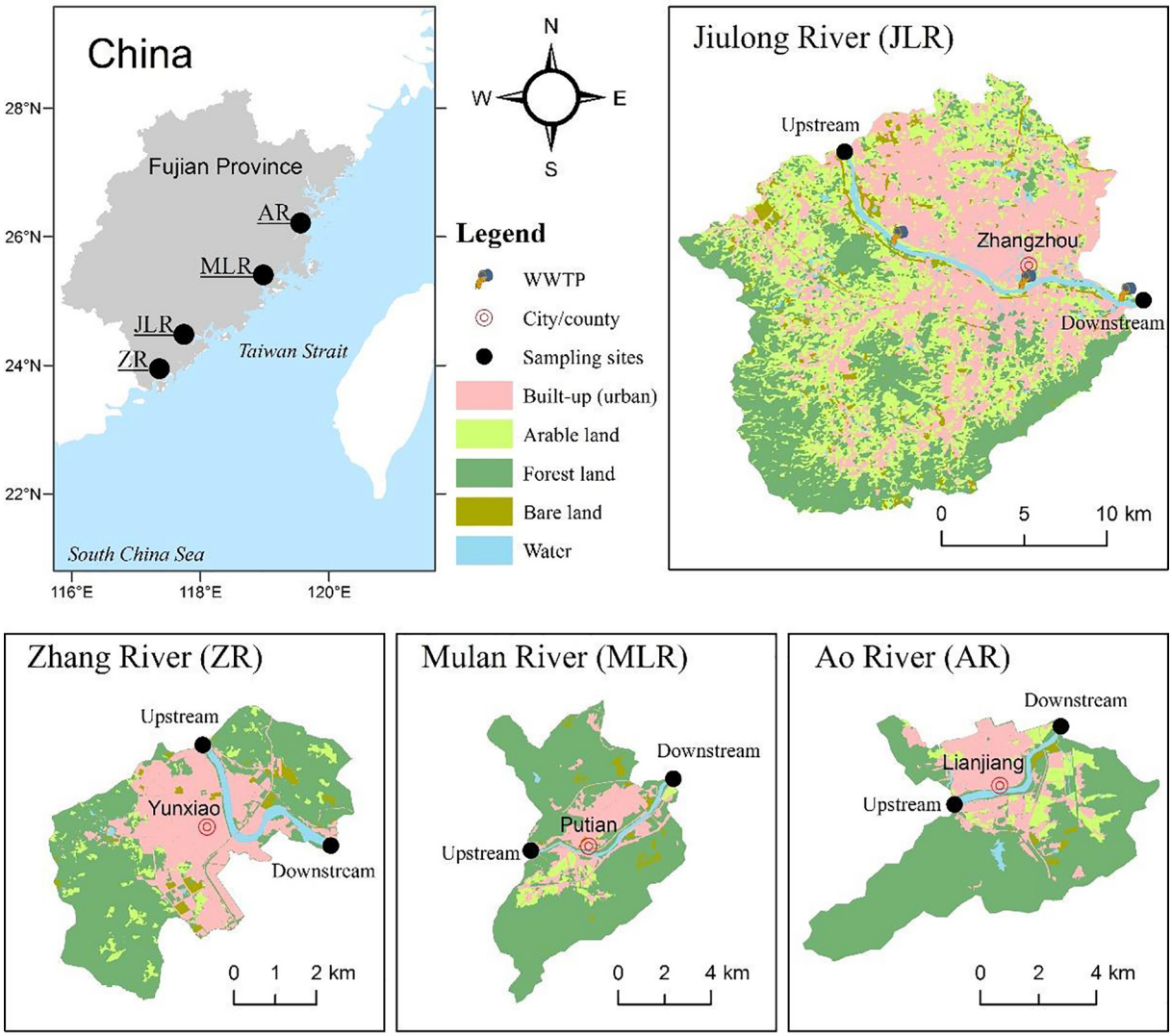

Fig. 1. Map of selected sections of urban rivers along the western coast of the Taiwan Strait, showing paired sampling sites (upstream versus downstream) for the urban area with various land uses. All rivers flow from west to east.

Table 1
Characteristics of selected parts of the urban rivers and land uses in the drainage area.

River (abbreviation)	Name of city	River reach (km)	Drainage (km^2)	Discharge (10^8 m^3)	Built-up (%)	Water (%)	Forest land (%)	Arable land (%)	Barren land (%)
Ao River (AR)	Lianjiang	11.2	45.09	8.17	19.2	2.6	69.7	7.2	1.1
Mulan River (MLR)	Putian	26.3	53.59	34.8	19.1	1.9	76.7	3.9	2.1
Jiulong River (JLR)	Zhangzhou	14.0	420.58	45.5	43.2	2.8	28.4	31.0	3.5
Zhang River (ZR)	Yunxiao	4.0	24.93	1.01	30.0	3.7	58.0	5.5	2.5

Note: Data is for urban river reach between paired sampling sties (refer to Fig. 1).

the field using a WTW multi-parameter portable meter (Multi 3430, Germany).

Water for dissolved gases analysis were introduced into 12 mL (N_2) Labco bottles, 60 mL (N_2O) and 120 mL (N_2O isotope) brown glass bottles through a silicone tube. After about 3+ volumes of water had overflowed from the bottle, a final concentration of 0.1% of $HgCl_2$ was added to stop microbial activity. The bottles were immediately capped without air space.

All water samples were stored in a cooler and delivered to the lab within hours for filtration and analysis. About 200 mL of water samples were filtered by a GF/F membrane and analyzed for nutrient concentrations and isotopic compositions. About 1 L of water samples for analysis of gene abundance were filtered by a 20 μm bluteau before filtration by a 0.22 μm Isopore TM Membrane (47 mm, Millipore, USA). The filters were stored at −80℃ in a freezer until DNA extraction was carried out.

2.3. Chemical analysis

Filters (GF/F) were frozen at −20 °C before analysis of total suspended particulates (TSM). All TSM weights were determined as the differences between the unfiltered and filtered GF/F membranes after oven-drying (105 °C) to constant weights. Filtrate was analyzed for dissolved nutrient concentrations by segmented flow automated colorimetry (San++ analyzer, Germany). Nutrients species determined were ammonium (NH_4^+-N), nitrite (NO_3^--N), nitrate (NO_2^--N), dissolved reactive phosphorus (DRP) and dissolved silica (DSi). TDN was determined as NO_3^--N following oxidization with 4% alkaline potassium persulfate. Dissolved inorganic N (DIN) was calculated as the sum of NH_4^+-N, NO_3^--N and NO_2^--N. Dissolved organic N (DON) was calculated by subtracting DIN from TDN. The precision for the nutrient components was estimated by repeated determination of 10% of the samples and the relative error was 2–5%.

Concentration of dissolved N_2 was measured by a membrane inlet mass spectrometry (MIMS) using the N_2:Ar ratio method (Chen et al., 2014b). Concentration of dissolved N_2O was measured by Gas Chromatograph (Agilent 7890A, US). Isotopic composition of nitrogen and oxygen ($\delta^{15}N$ and $\delta^{18}O$) in nitrate was determined by a denitrifier method (Casciotti et al., 2002; Sigman et al., 2001), in which nitrate was reduced to N_2O by denitrifying bacteria that lack N_2O-reductase activity, and isotopic compositions were measured by Isotope Ratio Mass Spectrometer (IRMS, Isoprime 100, UK). $\delta^{15}N$ and $\delta^{18}O$ analysis of dissolved N_2O was carried out using a trace gas preparation unit (Precon, Finnigan, Germany) coupled to IRMS (Delta V, Finnigan, Germany). Site-preference (SP), the site-specific distribution of ^{15}N-N_2O, was calculated as the difference of $\delta15N_\alpha$ and $\delta15N_\beta$ (Toyoda and Yoshida, 1999). SP can be used to distinguish the source of N_2O from nitrification and incomplete denitrification (Decock and Six, 2013). Isotope analysis was only carried out in the LF and MF periods.

2.4. Molecular analysis

DNA extraction from the filter (Isopore™) was performed by FastDNA™ Spin Kit for Soil (Millipore, USA), suspended in 80 μL TE solution and stored at −80 °C until analysis. Concentration and purity of the DNA was quantified by the Nano Drop spectrophotometer (DN-1000; Isogen Life Science, the Netherlands).

The Arch-amoAF and Arch-amoAR primers targeted *amoA* (AOA) gene with 634 base pairs (bp) (Francis et al., 2005). *amoA* (AOB) (491 bp) was quantified using amoA2F and amoA2R primers (Rotthauwe et al., 1997). The nitrite-oxidizing bacteria *nxrA* primers (F1370 F1/F2843 R2) allows amplification of a 323-bp fragment (Wertz et al., 2008). The *narG* primers (1960m2f/2050m2r) were designed to amplify a 109 bp narG fragment from nitrate-reducing bacteria (Lopez-Gutierrez et al., 2004). The *nirS* primers (cd3Af/R3cd) were designed to extract a 411 bp fragment (Throback et al., 2004).

All N functional gene abundances were quantified by a Bio-Rad CFX96 qPCR in triplicates with three negative controls (no DNA template) and five standards. Each sample received 10 μL of Hieff™ SYBR Master Mix (Yeasen, China), 0.4*2 μL of primer, 1 μL of template DNA and 8.2 μL of ddH_2O.

2.5. Data analysis and statistics

Net denitrification product (excess N_2, or $\triangle N_2$) was calculated by equation (1); see more details in our previous study (Chen et al., 2014b).

$$\text{Excess } N_2 = [N_2{:}Ar]_{measured} * [Ar]_{expected} - [N_2]_{expected} \quad (1)$$

where $[N_2{:}Ar]_{measured}$ is the measured concentration (μmol L^{-1}) ratio of N_2:Ar, calibrated using five air-equilibrated water standards; $[Ar]_{expected}$ and $[N_2]_{expected}$ are the concentrations when the water is in equilibrium with the atmosphere (Weiss, 1970).

In order to distinguish the source of N_2O, the contribution of nitrification (f_N) and denitrification (f_D) to the total N_2O (N_2O_{total}) was calculated by equation (2) (Decock and Six, 2013).

$$\begin{cases} f_D = N_2O_D/N_2O_{total} \\ f_D = (SP_{total} - SP_N)/(SP_D - SP_N) \\ f_N = 1 - f_D \end{cases} \quad (2)$$

where SP_D and SP_N are the SP values observed for N_2O_D (denitrification) and N_2O_N (nitrification) in pure cultures; SP_{total} is the SP values measured for N_2O_{total} in the environmental sample; f is the fraction of remaining substrate. SP_N (32.8 ± 4.0‰) and SP_D (−1.6 ± 3.8‰) are microbial cultures and reactions with pure cultures.

Stable isotope analysis based on the SIAR model (Eq. (3)) was performed using *R* statistical software (Parnell et al., 2010) to estimate proportional contributions of four nitrate N sources, i.e. atmospheric deposition (AD), manure and sewage (M&S), soil organic N (NS) and fertilizer N (FN). $\delta^{15}N\text{-}NO_3^-$ and $\delta^{18}O\text{-}NO_3^-$ of each source were adapted from a previous study around the study area (Zhang et al., 2018).

$$\begin{cases} X_{ij} = \sum_{k=1}^{k} p_k C_{jk} + S_{jk} + \varepsilon_{jk} \\ S_{jk} \tilde{N}(\mu_{jk}, \omega_{jk}^2) \\ C_{jk} \tilde{N}(\lambda_{jk}, \tau_{jk}^2) \\ \varepsilon_{jk} \tilde{N}0, \ \sigma_j^2 \end{cases} \quad (3)$$

where X_{ij} is the isotope value j of the mixture i (i = 1, 2, 3, …, N and

j = 1, 2, 3, …, J); S_{jk} is the source value k based on isotope j (k = 1, 2, 3, …, K); μ_{jk} is mean value; ${\omega_{jk}}^2$ is standard deviation; p_k is the proportion of source k; c_{jk} is the fractionation factor for isotope j on source k; λ_{jk} is the mean distributed value; τ_{jk} is standard deviation; and ε_{ij} is the residual error (mean value 0 and standard deviation σ_j).

Apparent N retention within the urban river reach, AR (%) of each species was defined as the percentage difference of concentration at the downstream site (C_{DS}) from the upstream site (C_{US}) (Eq. (4)). Urbanization increases or decreases riverine N fluxes to coastal water when the AR value is positive or negative, respectively.

$$AR\,(\%) = (C_{DS} - C_{US})/C_{US} \times 100 \quad (4)$$

Correlation analysis and ANOVA ($p < 0.05$) was performed using SPSS 18.0 software. Redundancy analysis (RDA) was performed using *R* software to examine the possible associations between environmental factors and N functional genes in different river sites.

3. Results

3.1. Changes in physicochemistry and nitrogen species from upstream to downstream

Water temperatures, DO, pH and TSM varied from the upstream site (US) to downstream site (DS) under low flow (LF), medium flow (MF) and high flow (HF) conditions (Table 2). Water temperature changed little from US to DS but it was warmer in HF (32.5 °C) than LF (23.7 °C) and MF (26.9 °C). Average DO decreased by 15% ± 15% from US to DS, except JLR and ZR in MF (DO increased 49% and 61%, respectively). pH at DS was 4% ± 4% higher than US except ZR in HF (decreased 7%). TSM increased from US (44.3 ± 78.6 mg L^{-1}) to DS (121.4 ± 229.3 mg L^{-1}), especially in LF and MF (increased 163% and 135%, respectively).

Nutrient concentrations and fractions also changed through the urban areas (Table 2, Fig. 2). Average NH_4^+-N and the fraction of TDN at DS (41.4 μmol L^{-1} and 16%) were much higher than US (28.8 μmol L^{-1} and 10%), including an extreme case where the LF fraction increased by a factor of 13.4 ($p < 0.05$). Average NO_3^--N and the fraction at DS (147.2 μmol L^{-1} and 72%) were lower than US (165.2 μmol L^{-1} and 74%), except JLR (HF) where an increase of 55% was observed. Average NO_2^--N and fraction increased from US to DS. Overall, average DIN, DON and DTN concentrations at DS were higher than US. AR_{DRP}, AR_{DOP} and AR_{DTP} were 36%, 1% and 12%, respectively. The DRP fraction of TDP at DS sites increased 59%, while the DOP fraction decreased 9% compared with US. DSi was relatively stable across the two sites (Table 2).

The DIN:DRP:DSi ratios show that all measurements fell in the P-limited range (Fig. 3). The DIN:DRP ratio decreased from US (153:1) to DS (139:1), except in HF (Fig. 3a), and the average DSi:DIN ratio decreased from US (1.89:1) to DS (1.70:1), due to relatively more DIN addition (Fig. 3b).

Dissolved N_2 and N_2O also changed between US and DS (Fig. 4). In most cases ΔN_2 increased from US (15.56 ± 11.35 μmol L^{-1}) to DS (16.82 ± 6.53 μmol L^{-1}), and the largest AR_{N_2} (42%) was found in LF (Table 3). AR_{N_2O} was 51% (LF), 38% (MF), and 16% (HF), and its concentration peaked in LF (Table 3, Fig. 4b). The average ratio of ΔN_2O to ΔN_2 was slightly higher at DS sites (3.01‰ ± 1.82‰) than US (2.60‰ ± 1.44‰), except the negative AR_{N_2O/N_2} in HF (Table 3, Fig. 4c). The intramolecular distribution of ^{15}N-N_2O showed that the SP value decreased from US (25.47 ± 5.68) to DS (21.23 ± 3.77) (Fig. 4d). The fraction of nitrification-derived N_2O (f_N) was lower at DS under MF condition (Fig. 4e), while there was no significant difference under LF conditions.

Dual isotope composition and SIAR model outputs showed that the main sources of nitrate in urban rivers were sewage (M&S), followed by soil organic N (NS) and fertilizer (NF) (Fig. 5). Total contribution of M&S to the nitrate pool increased from 50% (mode) at US to 60% (mode) at

Table 2
Physicochemistry, nutrient concentration and fraction (mean ± SD) at the upstream and downstream site of urban rivers.

Parameter (unit)	Upstream site				Downstream site				Apparent Retention (%)			
	Low flow	Middle flow	High flow	Mean	Low flow	Middle flow	High flow	Mean	Low flow	Middle flow	High flow	Mean
T (°C)	23.9 ± 2.0	26.5 ± 2.2	32.7 ± 0.9	27.7 ± 4.2	23.4 ± 1.7	27.2 ± 1.5	32.5 ± 1.3	27.7 ± 4.2	−2 ± 5	3 ± 3	−1 ± 2	0 ± 4
DO (mg/L)	9.0 ± 3.0	6.2 ± 1.4	9.7 ± 1.9	8.3 ± 2.7	6.8 ± 1.6	6.9 ± 2.0	8.8 ± 1.9	7.5 ± 1.9	−20 ± 20	18 ± 45	−8 ± 11	−3 ± 31
pH	6.5 ± 0.2	6.9 ± 0.2	8.0 ± 0.8	7.1 ± 0.8	6.8 ± 0.3	7.3 ± 0.4	8.0 ± 0.7	7.4 ± 0.7	4 ± 3	6 ± 6	0 ± 5	3 ± 5
TSM (mg/L)	82 ± 131	43 ± 43	9 ± 3	44 ± 79	227 ± 356	120 ± 191	17 ± 13	121 ± 229	163 ± 272	135 ± 183	82 ± 85	127 ± 180
NH_4-N (μmol L^{-1})	5 ± 4	63 ± 42	18 ± 34	29 ± 39	35 ± 20	72 ± 45	17 ± 25	41 ± 37	1324 ± 1951*	83 ± 140	431 ± 330	613 ± 1171
NO_3-N (μmol L^{-1})	205 ± 96	189 ± 87	165 ± 85	165 ± 55	190 ± 77	133 ± 60	119 ± 62	147 ± 69	−1 ± 18	−21 ± 37	14 ± 28	−3 ± 30
NO_2-N (μmol L^{-1})	4 ± 2	18 ± 12	6 ± 5	9 ± 10	8 ± 4	14 ± 4	8 ± 7	10 ± 6	139 ± 94	54 ± 159	28 ± 22	74 ± 109
DIN (μmol L^{-1})	214 ± 98	270 ± 131	126 ± 66	203 ± 111	234 ± 95	234 ± 95	144 ± 75	199 ± 90	14 ± 13	−3 ± 49	16 ± 30	9 ± 32
DON (μmol L^{-1})	13 ± 3	37 ± 15	22 ± 12	25 ± 15	19 ± 10	43 ± 14	27 ± 16	30 ± 16	88 ± 33	23 ± 33	22 ± 18	41 ± 40
TDN (μmol L^{-1})	223 ± 107	306 ± 143	148 ± 77	226 ± 122	253 ± 105	261 ± 103	171 ± 91	228 ± 100	21 ± 19	0 ± 45	16 ± 27	12 ± 31
DRP (μmol L^{-1})	2 ± 1	3 ± 2	4 ± 3	2 ± 2	3 ± 1	3 ± 1	4 ± 4	3 ± 2	68 ± 51	29 ± 41	11 ± 21	36 ± 44
DSi (μmol L^{-1})	314 ± 28	226 ± 49	274 ± 61	271 ± 58	320 ± 24	233 ± 31	263 ± 45	272 ± 49	2 ± 5	5 ± 18	−3 ± 6	1 ± 11
NH_4-N/TDN (%)	3 ± 2	19 ± 8	8 ± 14	10 ± 11	13 ± 5	26 ± 11	8 ± 10	16 ± 11	1149 ± 1712*	65 ± 81	358 ± 310	524 ± 1028
NO_3-N/TDN (%)	93 ± 4	63 ± 8	74 ± 15	77 ± 16	76 ± 7	51 ± 12	72 ± 14	67 ± 15	−18 ± 5	−18 ± 22	−2 ± 2	−13 ± 14
NO_2-N/TDN (%)	2 ± 0	5 ± 3	3 ± 1	3 ± 2	4 ± 1	6 ± 1	4 ± 2	4 ± 2	94 ± 47	37 ± 80	13 ± 21	48 ± 61
DIN/TDN (%)	98 ± 6	87 ± 4	85 ± 4	90 ± 8	93 ± 2	83 ± 3	84 ± 2	87 ± 5	−5 ± 4	−4 ± 4	−1 ± 3	−3 ± 4
DON/TDN (%)	5 ± 1	13 ± 4	15 ± 4	11 ± 6	7 ± 2	17 ± 3	16 ± 2	13 ± 5	70 ± 31	32 ± 28	7 ± 20	33 ± 35
DRP/TDP (%)	60 ± 15	73 ± 15	48 ± 38	62 ± 25	74 ± 9	76 ± 7	62 ± 24	71 ± 15	19 ± 19	7 ± 21	151 ± 290	59 ± 167

Note: * significant different between upstream and downstream site ($p < 0.05$).

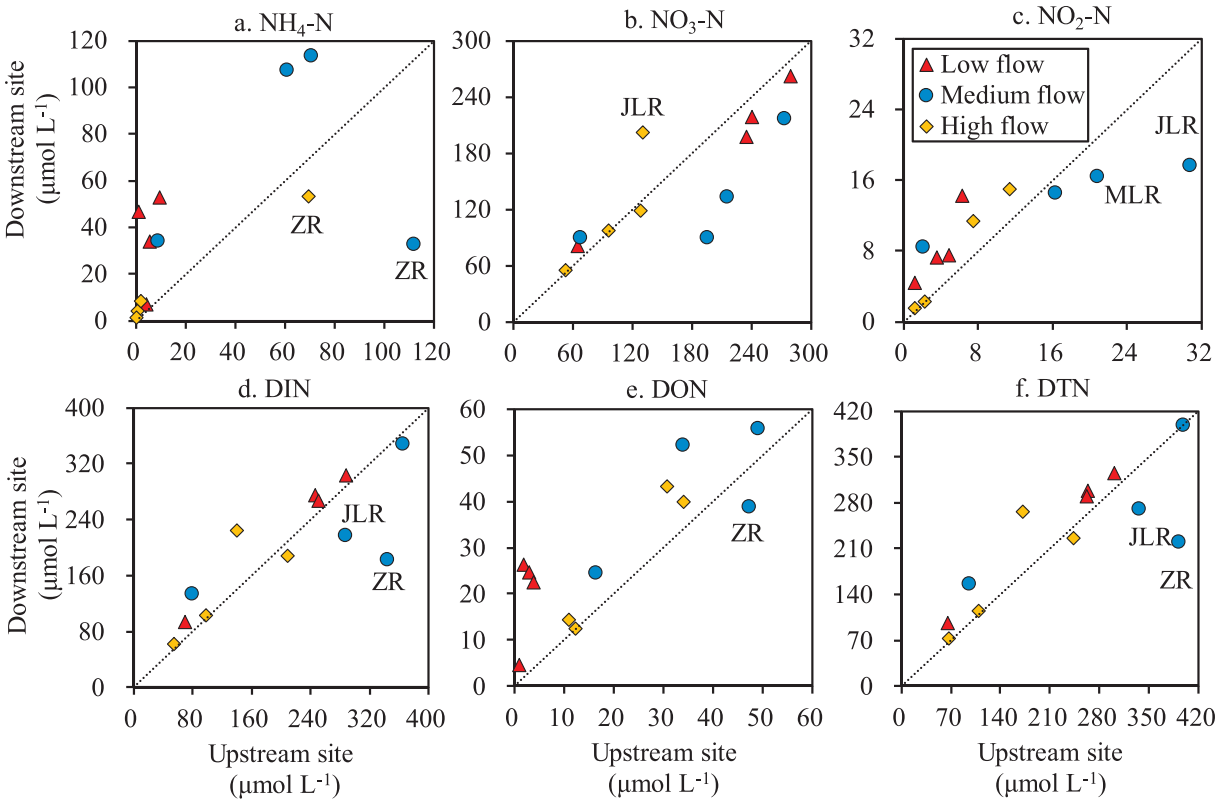

Fig. 2. Nutrient concentrations at downstream site (y-axis) against upstream site (x-axis) of four urban rivers under various flow conditions.

DS, although they varied between seasons (Table 4). In particular, the proportion of M&S was elevated even higher in MF than LF, whereas NS and NF contributed more in the high flow period (Table 4).

3.2. Abundance of nitrifying and denitrifying functional genes

The functional genes of nitrification (*amoA* and *nxrA*) and denitrification (*narG* and *nirS*) increased from US to DS, while a statistical difference was only observed for nxrA and narG in MF (Fig. 6). The abundance ratio of AOB to AOA was always greater than 1.0 but varied with flow conditions. The highest abundance was observed in MF. The average gene abundance was ordered as *nirS* (2.6×10^5 copies mL^{-1}) > *nxrA* (1.9×10^4 copies mL^{-1}) > *narG* (7.0×10^3 copies mL^{-1}) > AOB *amoA* (4.0×10^3 copies mL^{-1}) > AOA *amoA* (7.2×10^2 copies mL^{-1}), although it is difficult to directly assess the active role they played in N processes.

3.3. Relationships between environmental factors and nitrogen genes and retention

Internal relationships between environmental factors showed in the correlation heat map (Fig. 7). NH_4^+-N had a positive correlation with NO_2^--N ($r = 0.75$, $p < 0.01$) and ΔN_2 ($r = 0.69$, $p < 0.01$), and NO_3^--N and ΔN_2O were well correlated ($r = 0.5$, $p < 0.05$). NO_2^--N had a better relationship with ΔN_2 ($r = 0.82$, $p < 0.01$) than with ΔN_2O ($r = 0.61$, $p < 0.01$).

Redundancy analysis (RDA) was used to further examine possible associations between environmental factors and N functional gene abundance (Fig. 8). All the measured physicochemical parameters explained 75% of the variation in the five N functional genes among sites and over seasons. *amoA* of AOA and AOB was positively related with TSM, NH_4^+-N and NO_2^--N, but negatively related with pH. *narG* and *nxrA* had a positive relationship with TSM, NH_4^+-N, NO_2^--N and ΔN_2,

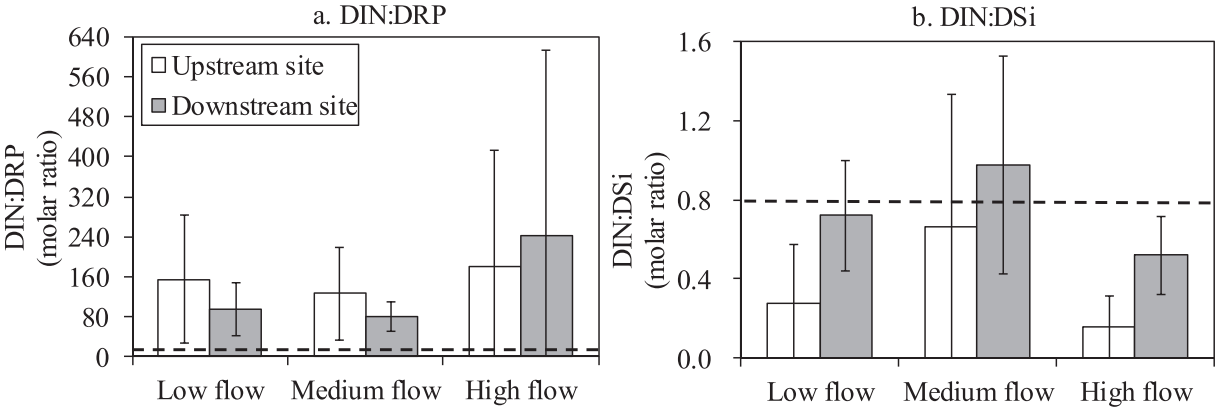

Fig. 3. Change in the DIN:DRP ratio and DIN:DSi ratio between upstream and downstream sites and among flow conditions. Column with error bar shows average and one standard deviation. Dashed lines indicate the Redfield molar ratio (DIN:DRP:DSi = 16:1:20).

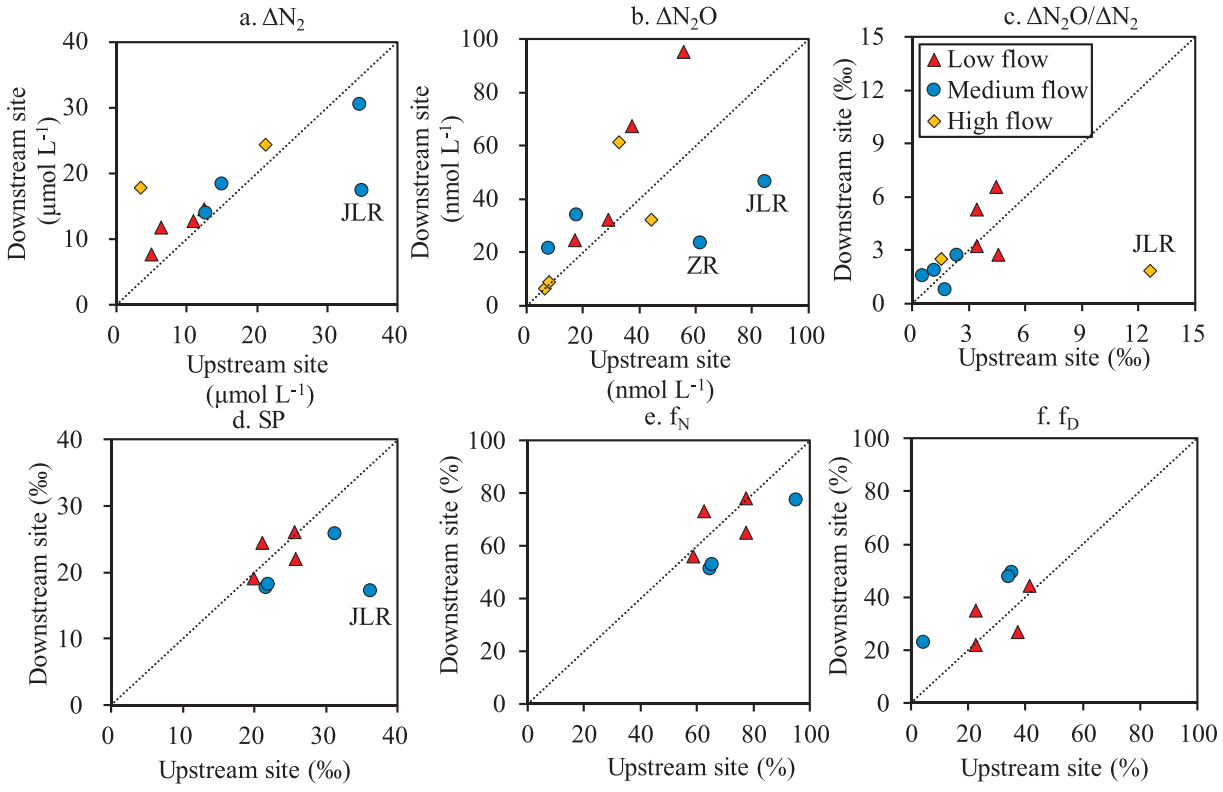

Fig. 4. The concentrations and ratio of ΔN_2, ΔN_2O and SP of N_2O at downstream site against upstream site. Site-preference (SP) was the site-specific distribution of ^{15}N-N_2O by calculated the difference of $\delta^{15}N_\alpha$ and $\delta^{15}N_\beta$. f_N means the fraction of nitrification-derived N_2O, and f_D the fraction of denitrification-derived N_2O.

Table 3
The apparent retention (%) (mean ± SD) of ΔN_2, ΔN_2O and $\Delta N_2O/\Delta N_2$.

Apparent Retention	Low flow	Middle flow	High flow
AR_{N_2}	42 ± 32	−8 ± 31	211 ± 278
AR_{N_2O}	51 ± 32	38 ± 112	16 ± 50
AR_{N_2O/N_2}	13 ± 45	40 ± 88	−11 ± 106

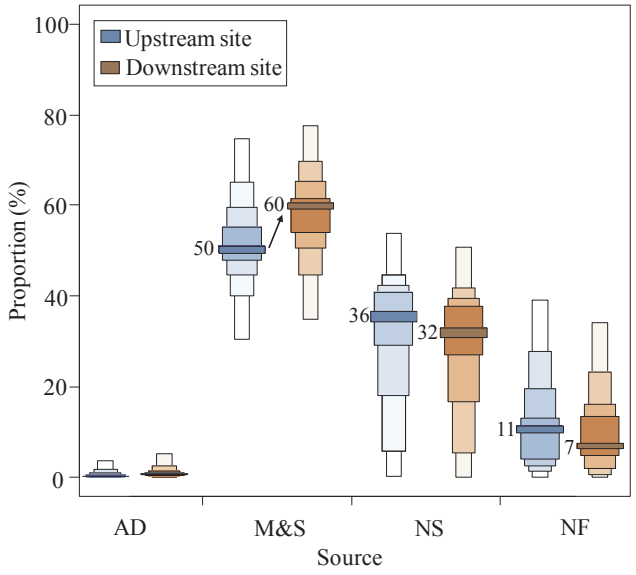

Fig. 5. The relative contribution of nitrate sources, i.e. atmospheric deposition (AD), manure and sewage (M&S), soil organic N (NS) and fertilizer N (NF). Box color from light to dark demarcates the 5th, 25th, 50th, 75th and 95th percentiles of probability.

but no relationship with NO_3^--N was found ($p > 0.05$). *nirS* was highly correlated with TSM, ΔN_2 and NO_2^--N ($p < 0.05$).

Correlations between apparent N retention within the urban river (AR, %) and land use in the drainage area (% of total area for each use, determined by satellite imagery) were explored. Most AR of N species had a weak relationship with land uses (data not shown), but AR_{N_2} had a strong negative correlation with built-up area in both LF ($r = -0.96$, $p < 0.05$) and MF ($r = -0.93$, $p > 0.05$) (Fig. 9).

4. Discussion

4.1. Urbanization increased nitrification and denitrification

A comparison of nitrogen concentration between US and DS suggests that the urban rivers received external NH_4^+-N loading as they passed through the urban area (Fig. 2). On average, NH_4^+-N concentration and its fraction of TDN increased from US to DS while nitrate decreased (Table 2), indicating relatively more NH_4^+-N input to rivers passing through urban areas. For each river, it received both raw sewage and effluent of WWTPs. The secondary effluent is characterized by high total N and low organic mater, with higher percentage of ammonium and nitrate (Simsek et al., 2012). Nitrate isotope signatures confirmed that sewage (M&S) was the dominant N source (Fig. 5), and its contribution increased from 50% at US sites to 60% at DS sites (Table 4). Not surprisingly, urban areas markedly increased ammonium loading to rivers.

The fate of ammonium N entering the fluvial system starts with nitrification. NH_4^+-N can be oxidized to nitrite by AOA and AOB and then to nitrate by the bacteria nxrA; nitrite can also be transformed to N_2O by NOB. AOB appears to play the primary role in ammonium oxidization, as its gene abundance (*amoA*) was far higher than AOA (Fig. 6). Unlike AOB, AOA might become important in low-nutrient, low-pH, and sulfide-containing environments (Erguder et al., 2009). Nitrite was found to have accumulated in these urban rivers (Fig. 2c),

Table 4
Proportional contribution (mean) of four potential nitrate sources in urban rivers estimated using SIAR mixing model.

Source	Low flow		Middle flow		Total	
	Upstream site	Downstream site	Upstream site	Downstream site	Upstream site	Downstream site
AD (%)	0.9	0.9	0.7	4.6	0.3	0.8
M&S (%)	43.2	46.2	39.6	47.8	50.2	59.9
NS (%)	28.3	28.2	33.6	33.7	35.6	31.9
NF (%)	6.2	5.7	25.1	15.0	10.5	7

Note: AD (atmospheric deposition), M&S (manure and sewage), NS (soil organic N) and NF (fertilizer N).

likely due to the greater microbial ammonia oxidation rate than nitrite oxidation rate (Hong et al., 2018). The functional gene *amoA* (AOA, AOB) *and nxrA* (NOB), and the nitrite-oxidizing bacteria *nxrA* generally increased from US to DS sites (Fig. 6), implying that urban rivers potentially enhanced nitrification. Average DO decreased by 15% from US to DS (Table 2), as expected due to nitrification-associated oxygen consumption.

River nitrate can be reduced to N_2O (a potent greenhouse gas) and N_2 via denitrification under anoxic condition (e.g. sediment-water interface, ground water and micro-environments in turbid water) (Beaulieu et al., 2011; Jahangir et al., 2013; Mulholland et al., 2008). A large number of studies suggest significant nitrate removal in river networks via denitrification (Chen et al., 2014a; Pina-Ochoa and Alvarez-Cobelas, 2006). In most cases, decreases in nitrate concentration and increases in $\triangle N_2O$ and $\triangle N_2$ were found at DS sites compared with US were observed (Fig. 2, Fig. 4). Apart from nitrification, N_2O can also be produced by nitrifier denitrification (Zhu et al., 2013). The increased ratio of ΔN_2O to ΔN_2 and decreased SP value of N_2O isotope (Fig. 4) suggest that more N_2O originated from denitrification in the downstream reaches of urban rivers, despite nitrification dominating N_2O production (Fig. 4e). As denitrifiers, the nitrate-reducing gene (*narG*) and nitrite-reducing gene (*nirS*) were more abundant at DS sites than US (Fig. 6). These results suggest that microbe-driven denitrification in urban rivers increased nitrate removal and greenhouse gases (N_2O) emission.

Here we further examine the major environmental factors controlling nitrification and denitrification in urban rivers. As shown in the correlation heat map (Fig. 7), there were statistically significant relationships between NH_4^+-N and NO_2^--N, NO_3^--N and ΔN_2O, and NO_2^--N and ΔN_2 ($p < 0.05$). The relationships, to some extent, reflect the importance of ammonium as a substrate in nitrification. Increased sewage ammonium loading to urban rivers should have stimulated nitrification. RDA shows that *amoA* (AOA and AOB), *nxrA*, *narG and nirS* were positively related with TSM ($p < 0.05$). In other words, TSM increased from US through DS and more suspended particles act as substrates for microorganisms (nitrifier and denitrifier) that facilitated nitrification and denitrification. In summary, urbanization increased nitrification and denitrification and gaseous N removal, but the strength varied with rivers and over seasons (see more discussion below).

4.2. Hydrological and meteorological controls on urban rivers regulating nitrogen retention and seaward export

Nitrogen levels in urban rivers are highly dynamic due to the combination of point source (e.g., sewage, wastewater treatment plant effluent) and non-point source pollution. Nitrogen loading was expected to increase with rainfall and urban runoff. Average NH_4^+-N concentration and its fraction of TDN were highest in MF both at US and DS sites. The first flush of land-based pollutants by surface runoff could explain this pattern (Mo et al., 2016). In contrast, the highest NO_3^--N was observed in LF, followed by MF and HF, as it mainly originated from ground water (baseflow) and can be diluted by increasing discharge (Gao et al., 2018). The contribution of NS (soil organic N) and NF (fertilizer N) to river N was greater in MF than LF (Table 4), suggesting hydrological controls on N loading to urban rivers.

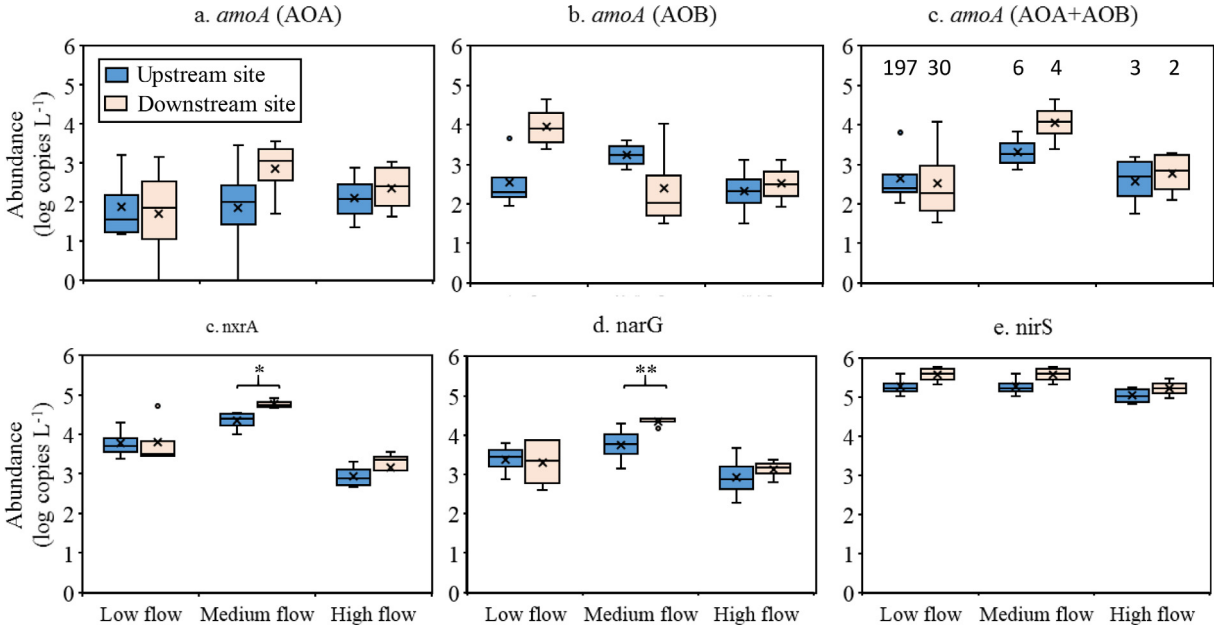

Fig. 6. Abundances of nitrifying and denitrifying functional genes in urban rivers. The number within panel c indicates the gene abundance ratio of AOB to AOA. Significant difference between upstream site and downstream site (*$p < 0.05$. **$p < 0.01$). Points indicate outlier and × is mean value.

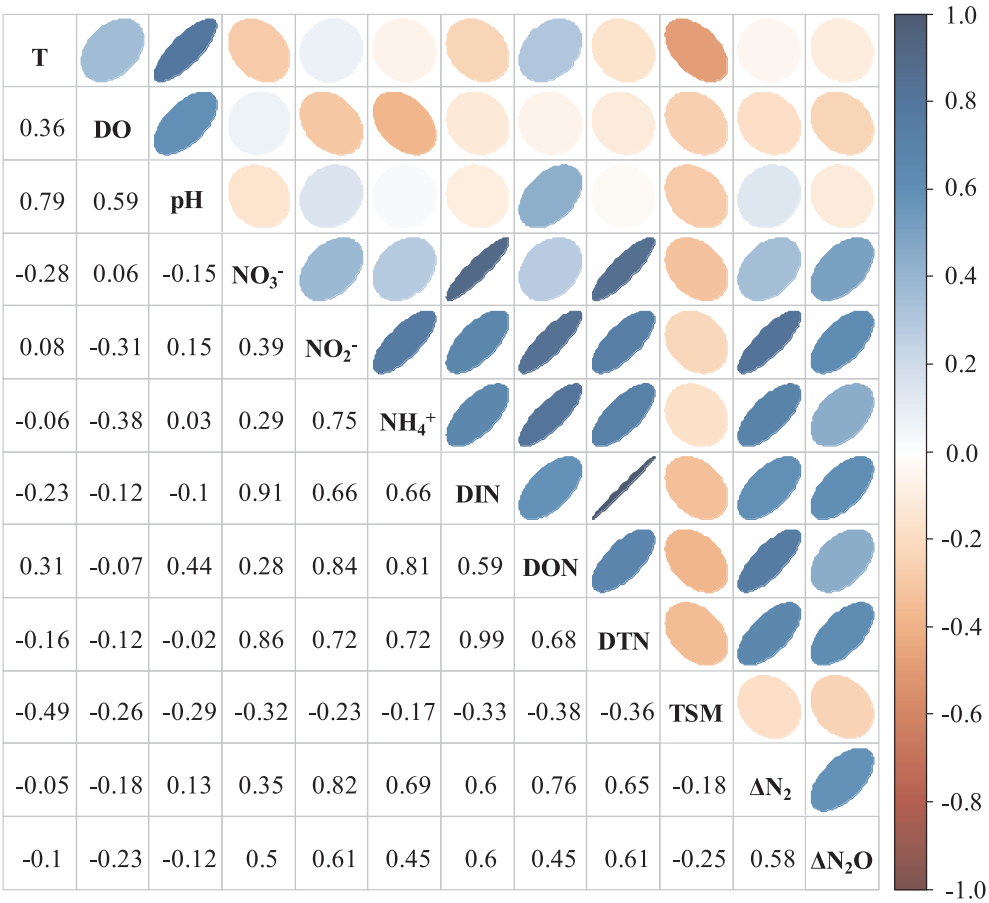

Fig. 7. Correlation heat map of environmental factors based on R software. The numbers show r value of correlation between groups. Blue shapes indicate a positive relationship and red indicates a negative relationship.

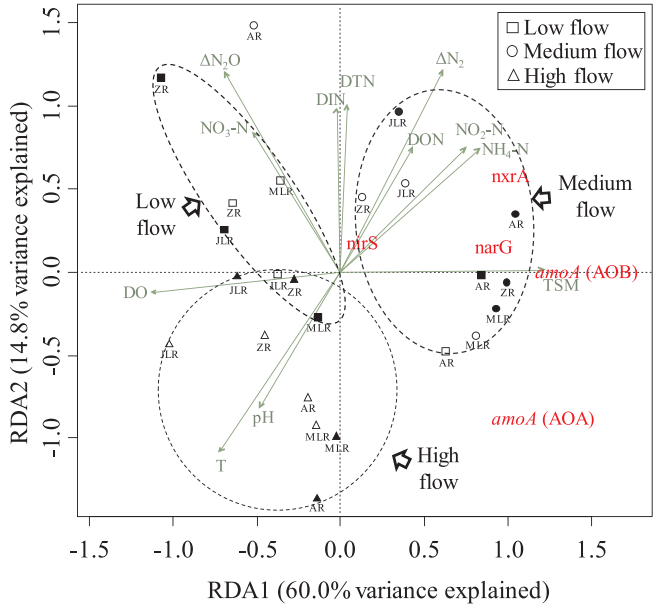

Fig. 8. Euclidean based redundancy analysis (RDA) of nitrogen functional genes and environmental factors. Outline symbols indicate upstream sites and solid symbols indicate downstream sites.

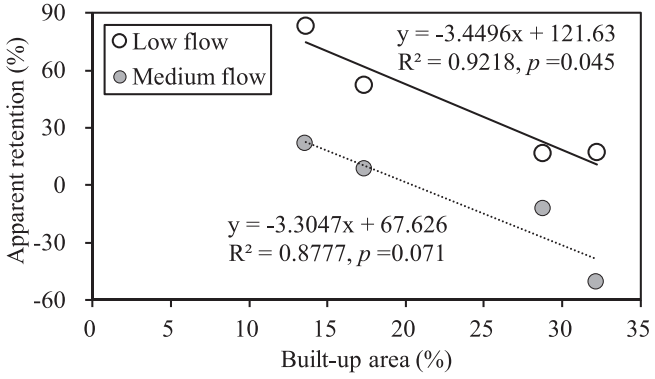

Fig. 9. Relationship between the apparent retention of N_2 from upstream to downstream site of urban rivers and the percentage of built-up area. High flow period measurements not shown as there was no relationship.

Biogeochemical cycling (within channel nitrification and denitrification) in urban rivers can be controlled by seasonal meteorological conditions since the growth and activity of microorganisms are sensitive to temperature (Sarker et al., 2013; Zheng et al., 2017). In this study, the abundance of nitrifying and denitrifying functional genes were mostly higher in MF than in LF and HF (Fig. 6). Optimum temperature (26.9 °C) and high substrate (rich in ammonium) in May 2018 (MF) resulted in stronger nitrification and ammonium removal. As low temperature and high flow (short water residence time) may have restrained nitrification (lower retention), ammonium increased more from US to DS in LF and HF periods compared with MF (Table 2).

Denitrification converts nitrate to gaseous N (e.g., N_2O, N_2) and therefore reduces the eutrophication problem. Although average nitrate concentration and fraction of TDN reduced much more from US to DS in MF compared with LF and HF, there was no consistent seasonal pattern of ΔN_2O and ΔN_2 (Fig. 4). The influence of temperature on

denitrification and N retention seems to vary widely between river systems. Low temperature and high flow may reduce denitrification as the lowest ΔN_2 was observed in LF and HF (Fig. 4). A previous study found that warming increased denitrification disproportionately due to altered oxygen dynamics (Veraart et al., 2011). In addition, seasonal changes in pH, TSM and other factors may also affect N functional genes and logically affect associated biological processes (Fig. 8). Proliferation of water hyacinth (*Eichhornia crassipes*) with large biological uptake in warm season, for example in the Zhang River (ZR) in MF period (Fig. S2), can also contribute to temporal retention of inorganic N forms (Fig. 2).

On average, retention of DIN and TDN in urban rivers was among highest under favorable conditions (MF) (Table 2). Nevertheless, river retention is limited given that DIN and TDN increased in most cases from US to DS. Furthermore, AR_{N_2} was negatively correlated with percentage of built-up area (Fig. 9), indicating that urban development will lower river N retention capacity. The relationships between urban watershed land use and water quality is complex (Carey et al., 2013), but current results suggest that increased nitrification and denitrification in urban rivers could not balance the large increase in urban N loading. In addition, the decreased DIN:DRP ratio and DIN:DSi ratio (because P increased even more quickly than N, Si changed little) in rivers passing through urban areas (Fig. 3) might reduce P limitation in aquatic ecosystems and favor HABs. In summary, urbanization increased anthropogenic N loading and seaward export with changing nutrient stoichiometry, which will likely exacerbate eutrophication in Chinese coastal waters.

5. Conclusions

Urban cities markedly increased N loading to rivers. The spatial pattern of N species (US versus DS) and isotope features revealed that urban sewage was the predominant source, although the contribution of non-point source pollution (soil N, fertilizer N) also increased in the high flow period. Ammonium N increased from US to DS with exceptions in some cases (e.g., large biological uptake). In contrast, nitrate mostly decreased along the urban rivers, and this was associated with increasing production of greenhouse gas N_2O and N_2 (end products of denitrification). Abundance of nitrifying and denitrifying functional genes and TSM increased in urban rivers and they are well correlated. Urbanization increased nitrification and denitrification and gaseous N removal.

Our results examined the hydrological and meteorological controls on urban rivers regulating N retention. Optimum temperature for nitrifiers and enrichment of ammonium (substrate) by surface runoff in MF might enhance nitrification. Marked nitrate removal occurred although many other factors can influence denitrification. Low temperature and high flow (short water residence time) likely reduced nitrification and denitrification. Urban development (larger built-up area) might lower river N retention (AR_{N_2}).

The increase in N retention by enhanced nitrification and denitrification in urban rivers could not balance the increase in anthropogenic N loading. The overall decreased DIN:DRP ratio and DIN:DSi ratio changed the nutrient supply to downstream aquatic ecosystems. Consequently, urbanization increased river N export and likely increased the potential for eutrophication.

Declaration of Competing Interest

The authors declare that they have no known competing financial interests or personal relationships that could have appeared to influence the work reported in this paper.

Acknowledgments

This research was supported by the National Key Research and Development Program of China (2016YFE0202100), and the National Natural Science Foundation of China (No. 41376082; 41676098). We thank Jing Yan and all peoples who assisted in sampling and lab analysis. We thank Michael Krom for his thoughtful comments. We thank Jonathan Vause for his assistance with English editing.

Appendix A. Supplementary data

Supplementary data to this article can be found online at https://doi.org/10.1016/j.ecolind.2019.105756.

References

Astaraie-Imani, M., Kapelan, Z., Fu, G.T., Butler, D., 2012. Assessing the combined effects of urbanisation and climate change on the river water quality in an integrated urban wastewater system in the UK. J. Environ. Manage. 112, 1–9.
Beaulieu, J.J., Tank, J.L., Hamilton, S.K., Wollheim, W.M., Hall, R.O., Mulholland, P.J., Peterson, B.J., Ashkenas, L.R., Cooper, L.W., Dahm, C.N., Dodds, W.K., Grimm, N.B., Johnson, S.L., McDowell, W.H., Poole, G.C., Valett, H.M., Arango, C.P., Bernot, M.J., Burgin, A.J., Crenshaw, C.L., Helton, A.M., Johnson, L.T., O'Brien, J.M., Potter, J.D., Sheibley, R.W., Sobota, D.J., Thomas, S.M., 2011. Nitrous oxide emission from denitrification in stream and river networks. Proc. Natl. Acad. Sci. U.S.A. 108, 214–219.
Carey, R.O., Hochmuth, G.J., Martinez, C.J., Boyer, T.H., Dukes, M.D., Toor, G.S., Cisar, J.L., 2013. Evaluating nutrient impacts in urban watersheds: challenges and research opportunities. Environ. Pollut. 173, 138–149.
Casciotti, K.L., Sigman, D.M., Hastings, M.G., Bohlke, J.K., Hilkert, A., 2002. Measurement of the oxygen isotopic composition of nitrate in seawater and freshwater using the denitrifier method. Anal. Chem. 74, 4905–4912.
Chen, N., Jiezhong, W.U., Chen, Z., Ting, L.U., Wang, L., 2014a. Spatial-temporal variation of dissolved N2 and denitrification in an agricultural river network, southeast China. Agric. Ecosyst. Environ. 189, 1–10.
Chen, N., Wu, J., Chen, Z., Lu, T., Wang, L., 2014b. Spatial-temporal variation of dissolved N-2 and denitrification in an agricultural river network, southeast China. Agric. Ecosyst. Environ. 189, 1–10.
Chen, N.W., Hong, H.S., 2012. Integrated management of nutrients from the watershed to coast in the subtropical region. Curr. Opin. Environ. Sustain. 4, 233–242.
Dalu, T., Wasserman, R.J., Magoro, M.L., Froneman, P.W., Weyl, O.L.F., 2019. River nutrient water and sediment measurements inform on nutrient retention, with implications for eutrophication. Sci. Total Environ. 684, 296–302.
de Andres, M., Barragan, J.M., Sanabria, J.G., 2017. Relationships between coastal urbanization and ecosystems in Spain. Cities 68, 8–17.
Decock, C., Six, J., 2013. How reliable is the intramolecular distribution of N-15 in N2O to source partition N2O emitted from soil? Soil Biol. Biochem. 65, 114–127.
Ding, J., Jiang, Y., Liu, Q., Hou, Z.J., Liao, J.Y., Fu, L., Peng, Q.Z., 2016. Influences of the land use pattern on water quality in low-order streams of the Dongjiang River basin, China: a multi-scale analysis. Sci. Total Environ. 551, 205–216.
Duh, J.D., Shandas, V., Chang, H., George, L.A., 2008. Rates of urbanisation and the resiliency of air and water quality. Sci. Total Environ. 400, 238–256.
Duha, J.D., Shandas, V., Chang, H.J., George, L.A., 2008. Rates of urbanisation and the resiliency of air and water quality. Sci. Total Environ. 400, 238–256.
Erguder, T.H., Boon, N., Wittebolle, L., Marzorati, M., Verstraete, W., 2009. Environmental factors shaping the ecological niches of ammonia-oxidizing archaea. FEMS Microbiol. Rev. 33, 855–869.
FAO, F., 2018. Yearbook 2018. Food and Agriculture Organization of the United Nations.
Francis, C.A., Roberts, K.J., Beman, J.M., Santoro, A.E., Oakley, B.B., 2005. Ubiquity and diversity of ammonia-oxidizing archaea in water columns and sediments of the ocean. Proc. Natl. Acad. Sci. U.S.A. 102, 14683–14688.
Gao, X.J., Chen, N.W., Yu, D., Wu, Y.Q., Huang, B.Q., 2018. Hydrological controls on nitrogen (ammonium versus nitrate) fluxes from river to coast in a subtropical region: observation and modeling. J. Environ. Manage. 213, 382–391.
Grimm, N.B., Faeth, S.H., Golubiewski, N.E., Redman, C.L., Wu, J.G., Bai, X.M., Briggs, J.M., 2008. Global change and the ecology of cities. Science 319, 756–760.
Gu, B.J., Dong, X.L., Peng, C.H., Luo, W.D., Chang, J., Ge, Y., 2012. The long-term impact of urbanization on nitrogen patterns and dynamics in Shanghai, China. Environ. Pollut. 171, 30–37.
Hobbie, S.E., Finlay, J.C., Janke, B.D., Nidzgorski, D.A., Millet, D.B., Baker, L.A., 2017. Contrasting nitrogen and phosphorus budgets in urban watersheds and implications for managing urban water pollution. Proc. Natl. Acad. Sci. U.S.A. 114, 4177 E4116-E4116.
Hong, Y., Wang, Y., Wu, J., Jiao, L., He, X., Wen, X., Zhang, H., Chang, X., 2018. Developing a mathematical modeling method for determining the potential rates of microbial ammonia oxidation and nitrite oxidation in environmental samples. Int. Biodeterior. Biodegrad. 133, 116–123.
Jahangir, M.M.R., Johnston, P., Barrett, M., Khalil, M.I., Groffman, P.M., Boeckx, P., Fenton, O., Murphy, J., Richards, K.G., 2013. Denitrification and indirect N2O emissions in groundwater: hydrologic and biogeochemical influences. J. Contam. Hydrol. 152, 70–81.
Li, K., 2018. Chinese Government Report. The 13th National People's Congress of China.
Lopez-Gutierrez, J.C., Henry, S., Hallet, S., Martin-Laurent, F., Catroux, G., Philippot, L., 2004. Quantification of a novel group of nitrate-reducing bacteria in the environment by real-time PCR. J. Microbiol. Methods 57, 399–407.
Marce, R., von Schiller, D., Aguilera, R., Marti, E., Bernal, S., 2018. Contribution of

hydrologic opportunity and biogeochemical reactivity to the variability of nutrient retention in river networks. Glob. Biogeochem. Cycle 32, 376–388.
Mo, Q., Chen, N., Zhou, X., Chen, J., Duan, S., 2016. Ammonium and phosphate enrichment across the dry-wet transition and their ecological relevance in a subtropical reservoir, China. Environ. Sci. Process Impacts 18, 882–894.
Mulholland, P.J., Helton, A.M., Poole, G.C., Hall, R.O., Hamilton, S.K., Peterson, B.J., Tank, J.L., Ashkenas, L.R., Cooper, L.W., Dahm, C.N., Dodds, W.K., Findlay, S.E.G., Gregory, S.V., Grimm, N.B., Johnson, S.L., McDowell, W.H., Meyer, J.L., Valett, H.M., Webster, J.R., Arango, C.P., Beaulieu, J.J., Bernot, M.J., Burgin, A.J., Crenshaw, C.L., Johnson, L.T., Niederlehner, B.R., O'Brien, J.M., Potter, J.D., Sheibley, R.W., Sobota, D.J., Thomas, S.M., 2008. Stream denitrification across biomes and its response to anthropogenic nitrate loading. Nature 452, 202–U246.
Paerl, H.W., Gardner, W.S., Havens, K.E., Joyner, A.R., McCarthy, M.J., Newell, S.E., Qin, B.Q., Scott, J.T., 2016. Mitigating cyanobacterial harmful algal blooms in aquatic ecosystems impacted by climate change and anthropogenic nutrients. Harmful Algae 54, 213–222.
Panthi, J., Li, F., Wang, H., Aryal, S., Dahal, P., Ghimire, S., Kabenge, M., 2017. Evaluating climatic and non-climatic stresses for declining surface water quality in Bagmati River of Nepal. Environ. Monit. Assess. 189.
Parnell, A.C., Inger, R., Bearhop, S., Jackson, A.L., 2010. Source partitioning using stable isotopes: coping with too much variation. PLoS ONE 5.
Pernet-Coudrier, B., Qi, W.X., Liu, H.J., Muller, B., Berg, M., 2012. Sources and pathways of nutrients in the semi-arid region of Beijing Tianjin, China. Environ. Sci. Technol. 46, 5294–5301.
Pina-Ochoa, E., Alvarez-Cobelas, M., 2006. Denitrification in aquatic environments: a cross-system analysis. Biogeochemistry 81, 111–130.
Rotthauwe, J.H., Witzel, K.P., Werner, Liesack, 1997. The ammonia monooxygenase structural gene amoA as a functional marker: molecular fine-scale analysis of natural ammonia-oxidizing populations. Appl. Environ. Microl. 63, 4704–4712.
Sarker, D.C., Sathasivan, A., Joll, C.A., Heitz, A., 2013. Modelling temperature effects on ammonia-oxidising bacterial biostability in chloraminated systems. Sci. Total Environ. 454, 88–98.
Seto, K.C., Fragkias, M., 2005. Quantifying spatiotemporal patterns of urban land-use change in four cities of China with time series landscape metrics. Landscape Ecol. 20, 871–888.
Sigman, D.M., Casciotti, K.L., Andreani, M., Barford, C., Galanter, M., Bohlke, J.K., 2001. A bacterial method for the nitrogen isotopic analysis of nitrate in seawater and freshwater. Anal. Chem. 73 (17), 4145–4153. https://doi.org/10.1021/ac010088e.
Simsek, H., Kasi, M., Wadhawan, T., Bye, C., Blonigen, M., Khan, E., 2012. Fate of dissolved organic nitrogen in two stage trickling filter process. Water Res. 46, 5115–5126.
Throback, I.N., Enwall, K., Jarvis, A., Hallin, S., 2004. Reassessing PCR primers targeting nirS, nirK and nosZ genes for community surveys of denitrifying bacteria with DGGE. FEMS Microbiol. Ecol. 49, 401–417.
Toyoda, S., Yoshida, N., 1999. Determination of nitrogen isotopomers of nitrous oxide on a modified isotope ratio mass spectrometer. Anal. Chem. 71, 4711–4718.
Veraart, A.J., de Klein, J.J.M., Scheffer, M., 2011. Warming can boost denitrification disproportionately due to altered oxygen dynamics. PLoS ONE 6, 6.
Weiss, R.F., 1970. The solubility of nitrogen, oxygen and argon in water and seawater. Deep-Sea Res. Oceanographic Abstracts 17, 721–735.
Wertz, S., Poly, F., Le Roux, X., Degrange, V., 2008. Development and application of a PCR-denaturing gradient gel electrophoresis tool to study the diversity of Nitrobacter-like nxrA sequences in soil. FEMS Microbiol. Ecol. 63, 261–271.
Xian, C.F., Zhang, X.L., Zhang, J.J., Fan, Y.P., Zheng, H., Salzman, J., Ouyang, Z.Y., 2019. Recent patterns of anthropogenic reactive nitrogen emissions with urbanization in China: dynamics, major problems, and potential solutions. Sci. Total Environ. 656, 1071–1081.
Zhang, M., Zhi, Y., Shi, J., Wu, L., 2018. Apportionment and uncertainty analysis of nitrate sources based on the dual isotope approach and a Bayesian isotope mixing model at the watershed scale. Sci. Total Environ. 639, 1175–1187.
Zhang, W.S., Swaney, D.P., Hong, B.H., Howarth, R.W., Li, X.Y., 2017. Influence of rapid rural-urban population migration on riverine nitrogen pollution: perspective from ammonia-nitrogen. Environ. Sci. Pollut. Res. 24, 27201–27214.
Zhang, X.H., Wu, Y.Y., Gu, B.J., 2015. Urban rivers as hotspots of regional nitrogen pollution. Environ. Pollut. 205, 139–144.
Zheng, Z.Z., Wan, X.H., Xu, M.N., Hsiao, S.S.Y., Zhang, Y., Zheng, L.W., Wu, Y.H., Zou, W.B., Kao, S.J., 2017. Effects of temperature and particles on nitrification in a eutrophic coastal bay in southern China. J. Geophys. Res.-Biogeosci. 122, 2325–2337.
Zhu, X., Burger, M., Doane, T.A., Horwath, W.R., 2013. Ammonia oxidation pathways and nitrifier denitrification are significant sources of N2O and NO under low oxygen availability. Proc. Natl. Acad. Sci. U.S.A. 110, 6328–6333.